




Novel direct synthetic route of 2D Prussian Blue analogue, nanocrystalline CuHCF, as highly effective cathode materials for Zn-ion supercapacitors

Maria V. Kaneva , Anastasia K. Bachina , Artem A. Lobinsky* 

Ioffe Institute, Saint-Petersburg 194021, Russia

* Corresponding author: lobinski.a@mail.ru



This paper belongs to a Regular Issue.

Abstract

Prussian blue analogues (PBAs) with 2D morphology of nanocrystals have attracted much attention for aqueous electrolyte-based energy storage devices. In this study, we synthesized a 2D Prussian blue analogue, nanocrystals of copper hexacyanoferrate (CuHCF), via a facile stepwise route involving a modified copper substrate of Cu(OH)₂ nanorods that was used for the formation of two-dimensional CuHCF crystals. These materials were characterized by powder X-ray diffraction, energy dispersive X-ray microanalysis, X-ray photoelectron spectroscopy and scanning electron microscopy. The cathode based on 2D CuHCF exhibits high specific capacity (240 F/g (63.9 mAh/g) at 0.1 A/g) with excellent cycling stability (98.5% retention after 1000 charge-discharge cycles) in 3 M ZnSO₄ electrolyte. The flat two-dimensional morphology of CuHCF provides sufficient ion diffusion channels and the numerous electroactive interfaces for intercalation charge storage.

Keywords

Prussian blue analogue
transition metals
2D crystals
cathode materials
supercapacitors

Received: 21.11.23

Revised: 22.12.23

Accepted: 28.12.23

Available online: 31.12.23

© 2023, the Authors. This article is published in open access under the terms and conditions of the Creative Commons Attribution (CC BY) license (<http://creativecommons.org/licenses/by/4.0/>).

1. Introduction

Rechargeable metal-ion (Na, K, Mg, Zn) batteries are promising for replacing traditional power sources. They meet the requirements for highly efficient electrical energy storage devices because they possess high energy density, are environmentally friendly, safe, and inexpensive [1]. Among the most promising candidates for energy storage devices are hybrid zinc-ion supercapacitors (ZISCs), which combine batteries-type and supercapacitors-type electrodes. Among the metal ions used as charge carriers, zinc ions have the smallest radius and the highest electrode potential, which makes their use effective and safe in aqueous electrolytes [2]. ZISCs exhibited high power density, conductivity and fast charge-discharge process. However, there are still difficulties associated with the lack of suitable cathode materials that have a specific capacity close to theoretical and are capable of withstanding multiple intercalation/deintercalation of zinc ions [3]. Recently developed Zn-ion hybrid supercapacitors have demonstrated enhanced characteristics, including high energy density and specific power as well as long cycling

stability, which opens up prospects for their use in portable and micro-dimensional flexible devices [4, 5].

Hybrid zinc-ion supercapacitors are classified into two configurations depending on the electrode material. The first configuration of ZISCs consists of a Zn anode and a supercapacitor-type cathode, while the second configuration of ZISCs consists of a capacitor-type anode and a capacitive-type cathode [6–8].

Generally, supercapacitor-type electrodes are usually various carbon materials and MXenes. Battery-type electrodes are capacity and pseudocapacity materials such as manganese oxides, vanadium oxides, analogues of Prussian blue, etc [9].

Recently, compounds of transition metals (Cu, Ni, Co, Mn, etc.) based on Prussian Blue analogues (PBAs) have been of great interest due to their unique structural characteristics, including an open frame structure, high specific surface area and electrochemical activity as well as the possibility of flexible regulation of the number of active centers. They demonstrate possibilities for a wide range of applications as capacitive materials for supercapacitors [10, 11] and metal-ion batteries [12], efficient

electrocatalysts for water decomposition [13], electrochemical biosensors for the detection of glucose and hydrogen peroxide [14], etc.

In particular, copper-based PBAs (CuHCF) have shown high performance as electrode materials for metal-ion batteries and supercapacitors both in terms of specific capacity and cyclic stability [15–17]. However, PBAs are typically rather large cubic crystals that complicate the processes of ion diffusion and charge transfer. In addition, additional binding components (e.g., Nafion) must be used to apply PBAs powders on the electrode surface, which, in turn, slows down the conductivity and negatively affects performance [18]. Obtaining a PBAs crystal with two-dimensional (2D) morphology would be beneficial because of its high surface area, large number of active sites and ultra-thickness, which is conducive to charge transfer in materials [19–21].

Recent studies have shown the prospects of an approach to the synthesis of PBAs frameworks using the hydroxides of different transition metals as templates that react directly with metal hexacyanoferrate solution under "soft" conditions [22].

In this paper, we propose a fundamentally new technique for the synthesis of copper hexacyanoferrate on the surface of a modified copper substrate coated with a $\text{Cu}(\text{OH})_2$ layer by an exchange reaction between the $\text{Cu}(\text{OH})_2$ layer and $[\text{Fe}(\text{CN})_6]^{3-}$ in an aqueous solution of $\text{K}_3[\text{Fe}(\text{CN})_6]$. As a result, a set of two-dimensional CuHCF crystals with dimensions of 2–8 nm was formed on the surface of copper foam. The CuHCFs were studied as cathode materials for zinc-ion supercapacitors and demonstrated high performance.

2. Materials and Methods

2.1. Materials

Copper foam (80 PPI; size: 10×20 mm) was used as a substrate. For synthesis, we used copper sulfate pentahydrate ($\text{CuSO}_4 \cdot 5\text{H}_2\text{O}$), potassium persulfate ($\text{K}_2\text{S}_2\text{O}_8$), potassium ferrocyanide ($\text{K}_3[\text{Fe}(\text{CN})_6]$), and potassium hydroxide (KOH). All reagents were produced by LenReactiv (Russia).

2.2. Synthesis of 2D CuHCF nanocrystals

The copper foam (CF) was washed with acetone and deionized water (DI) under sonication for 10 min. At the first stage, the modification of the copper substrate was carried out by processing potassium persulfate in an alkaline solution with the formation of a $\text{Cu}(\text{OH})_2$ layer on the surface of CF. The pre-purified CF was immersed in a mixture of potassium persulfate (0.0235 g $\text{K}_2\text{S}_2\text{O}_8$ on 10 ml DI) and potassium hydroxide (1 g KOH on 10 ml DI) for 20 min and then washed several times with DI. Next, the substrate was immersed in 10 ml a 0.1 M

aqueous solution of $\text{K}_3[\text{Fe}(\text{CN})_6]$ for 24 h. Finally, the sample was washed several times in DI and dried in air for 24 h.

2.3. Characterisation

The morphology and element composition of synthesized samples were determined using a Tescan Vega 3 SBH microscope and an Oxford Instruments INCA x-act for energy-dispersive X-ray spectroscopy (EDX), respectively. X-ray photoelectron spectroscopy (XPS) was carried out using an ESCALAB 250Xi electron spectrometer.

Powder X-ray diffraction (PXRD) patterns were acquired employing a Rigaku SmartLab 3 diffractometer, utilizing $\text{Cu K}\alpha$ radiation. The data collection spanned an angular range from 5° to 100° in 2θ , with a step width of 0.01° , and a scan rate of $1^\circ/\text{min}$. The identification of phases was conducted through reference to the powder standard database, Inorganic Crystal Structure Database (ICSD). The determination of average crystallite size was performed using the Scherrer equation.

2.4. Electrochemical measurement

The electrochemical measurements were carried out using an Elins P-45X potentiostat/galvanostat (Elins, Russia) in a three-electrode electrochemical cell with Ag/AgCl electrode (reference), graphite rod electrode (counter), and the as-prepared samples (working electrode). 3M ZnSO_4 aqueous solution was used as an electrolyte.

3. Results and Discussion

The SEM image is shown in Figure 1. As can be clearly seen, on the surface of the copper foam there was the formation of a set of two-dimensional rectangular crystals with dimensions of 2–8 μm . The crystals are located mainly perpendicular to the surface of the substrate (Figure 1a). To determine the composition, EDX elements mapping was performed, which confirmed the presence of Cu, Fe and K elements in the composition of the sample (Figure 1b).

The X-ray diffraction measurements allowed determining the crystal structure of the sample obtained by a reaction with potassium hexacyanoferrate(III) $\text{K}_3[\text{Fe}(\text{CN})_6]$ on a copper foam substrate, in conjunction with pre-synthesized $\text{Cu}(\text{OH})_2$. The phase analysis results, depicted in Figure 2, reveals the coexistence of CuO, $\text{Cu}(\text{OH})_2$ (orthorhombic, Space Group: Cmc2), and $\text{K}_2\text{Cu}[\text{Fe}(\text{CN})_6]$. The latter compound, often referred to as a Prussian blue analogue, exhibits a triclinic structure (Space Group: P-1). The mass ratio of the phases is determined to be 39.5:7.5:53. The average crystallite size is measured at 29 ± 2 nm for CuO and 52 ± 2 nm for $\text{K}_2\text{Cu}[\text{Fe}(\text{CN})_6]$. A marginal presence of copper oxide, constituting 39.5 wt.%, was also detected. The potential source of copper oxide in the samples is likely attributable to the oxidation of copper in potassium ferrocyanide.

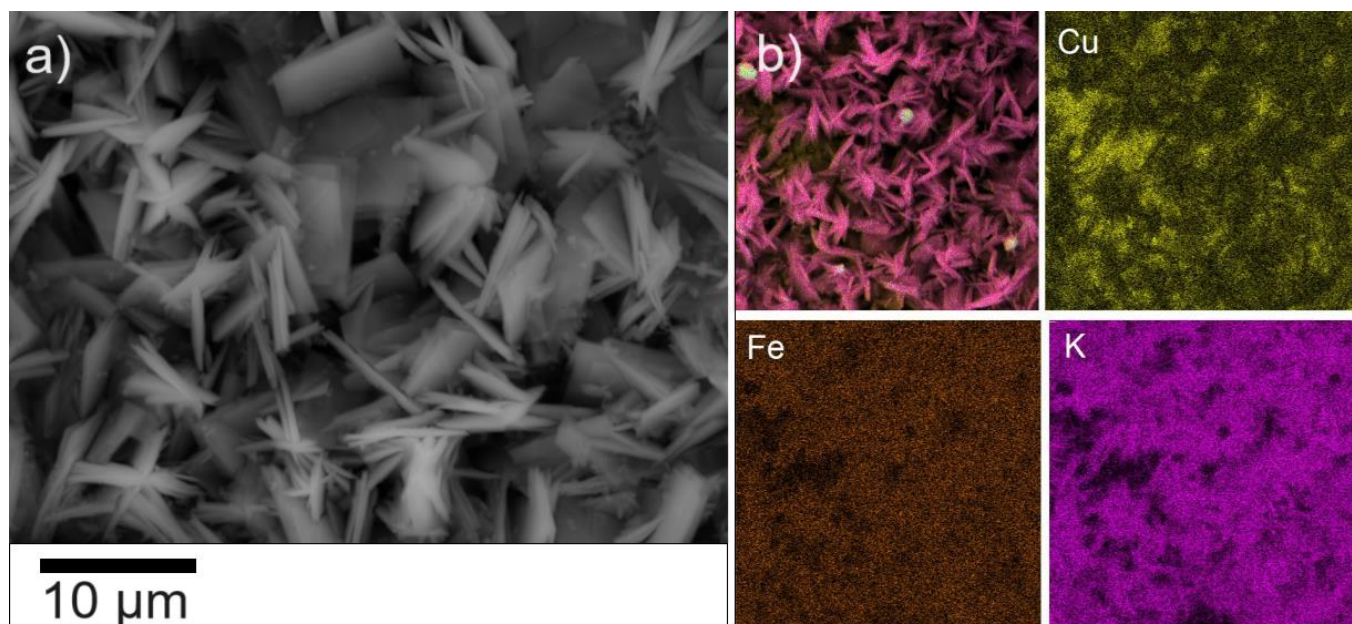


Figure 1 SEM images of 2D CuHCF nanocrystals (a) and EDX element mapping (Cu, Fe, K and mixed) of CuHCF (b).

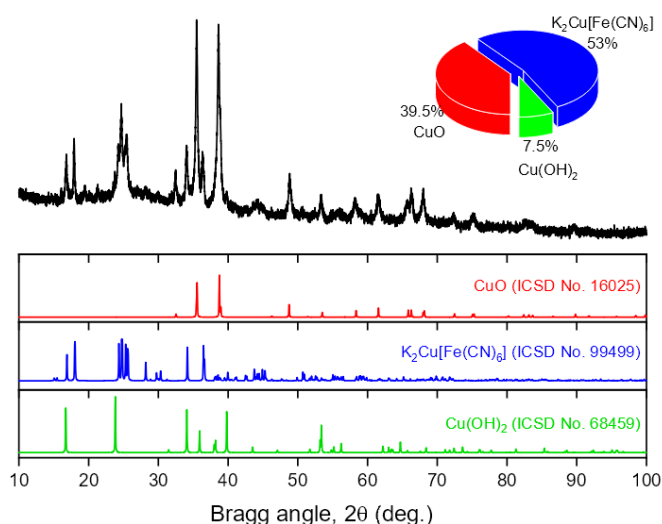


Figure 2 XRD pattern collected from the CuHCF sample, accompanied by the reference patterns from ICSD No. 16025, No. 99499, and No. 68459.

The XPS spectra of CuHCF are shown in Figure 3. The peaks with the binding energies of 934.4 eV and 954.5 eV in the Cu 2p spectrum likely correspond to Cu^{2+} atoms of CuHCF and CuO [23]. The peaks of Fe 2p with the binding energy of 707.8 eV and 720.5 eV correspond to Fe^{2+} in the hexacyanoferrate framework [23]. The presence of peaks of C 1s (284.3 eV) and N 1s (397.4 eV) in the XPS spectra confirms the formation $\text{K}_2\text{Cu}[\text{Fe}(\text{CN})_6]$ from $\text{Cu}(\text{OH})_2$.

Thus, two-dimensional crystals of $\text{K}_2\text{Cu}[\text{Fe}(\text{CN})_6]$ are formed as a result of the synthesis. At the same time, CuO and $\text{Cu}(\text{OH})_2$ phases formed during the previous stages of synthesis are preserved in the sample. Probably monoclinic $\text{Cu}(\text{OH})_2$ crystals obtained at the first stage of synthesis determine the further formation of the two-dimensional morphology of $\text{K}_2\text{Cu}[\text{Fe}(\text{CN})_6]$ crystals.

The electrochemical characteristics of CuHCF/CF as a cathode of Zn-ion supercapacitor were studied by the cycling voltammogram (CVA) and galvanostatic charge-discharge (GCD) technique. The measurements were carried out in an aqueous solution of 3 M ZnSO_4 .

Figure 4a exhibits CVA of CuHCF electrode at the scan rates of 5 mV/s, 10 mV/s, 15 and 20 mV/s in 0–1.0 V potential window. The broad anodic peak is located at 0.720 V, and the cathodic peak are centered at 0.580 V. This shows that the charge is stored by the reversible redox processes of $\text{Fe}^{3+}/\text{Fe}^{2+}$ in CuHCF/CF electrode [24].

The galvanostatic discharge curves at different current densities (0.1 A/g, 0.2 A/g, 1 A/g) are shown in Figure 4b. The specific capacity was calculated from the discharge curves according to the method described in [10]. The specific capacity of CuHCF was 240 F/g (63.9 mAh/g), 208 F/g (27.8 mAh/g), and 164 F/g (4.2 mAh/g) at the current density of 0.1 A/g, 0.2 A/g and 1 A/g, respectively. The cycle stability tests were carried out at the current density of 0.2 A/g. The capacity slightly decreases to 98.5% after 1000 charge-discharge cycles (see the inset in Figure 4b), indicating good reversibility of the processes.

4. Limitations

Within the framework of this work, the possibility of optimizing the synthesis conditions to obtain the best electrochemical characteristics was not considered. The ability to influence the morphology and size of the crystals formed can be achieved by changing the processing time and concentration of $\text{K}_3[\text{Fe}(\text{CN})_6]$, as well as by adjusting the thickness of the $\text{Cu}(\text{OH})_2$ layer by changing the processing time of the initial copper substrate in an alkaline solution of potassium persulfate.

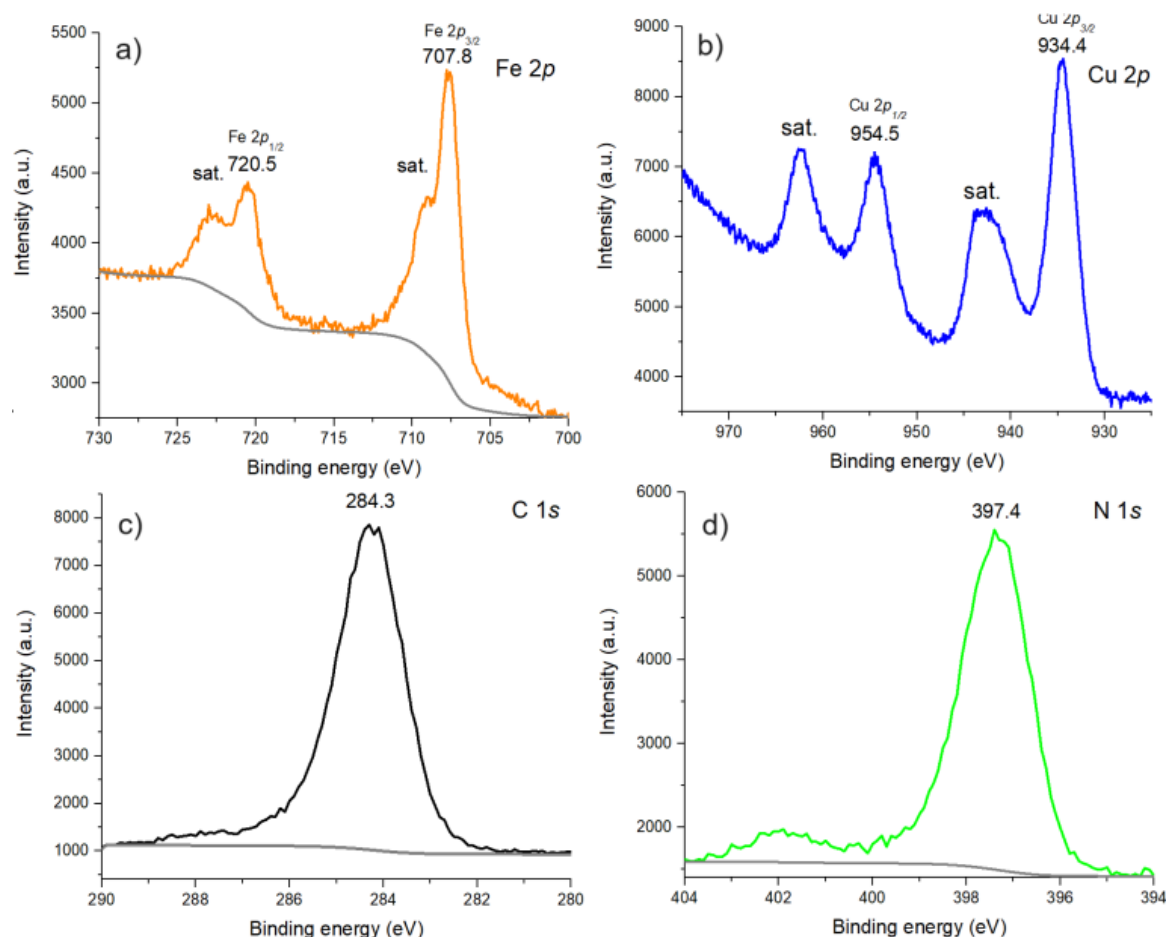


Figure 3 XPS spectra of CuHCF in Fe 2p (a), Cu 2p (b), C 1s (c) and N 1s (d) areas.

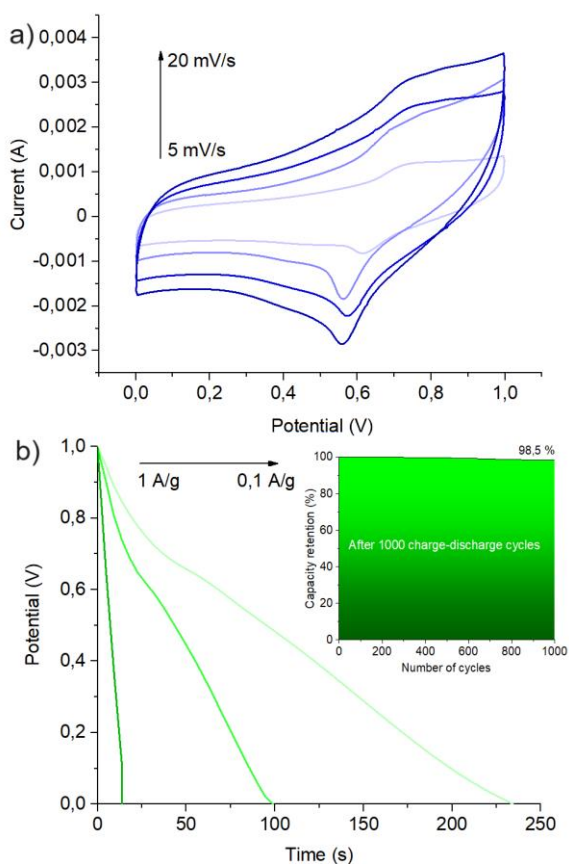


Figure 4 CVA curves (a) and discharge curves (b) of CuHCF/CF electrode. The inset (b) shows the cycling stability diagram.

5. Conclusions

Summing up, we demonstrated the possibility of the synthesis of 2D CuHCF by two-stage modification of copper foam under mild conditions. The synthesized material exhibited relatively high-capacity performance and excellent cycling stability in cathodes for a zinc-ion supercapacitor. The proposed synthesis strategy can be extended to obtain analogues of Prussian blue based on other transition metals. In addition, the proposed synthesis method is quite simple, cost-effective and easily scalable.

• Supplementary materials

No supplementary materials are available.

• Funding

This work was supported by the Russian Science Foundation (grant no. 22-23-20138)

• Acknowledgments

The authors gratefully acknowledge to the Centre for Physical Methods of Surface Investigation of St. Petersburg State University. The SEM and PXRD study were conducted utilizing equipment at the Engineering Center of the St. Petersburg State Institute of Technology.

● Author contributions

Conceptualization: A.A.L.

Data curation: A.A.L., M.V.K.

Formal Analysis: A.A.L., M.V.K., A.K.B.

Funding acquisition: A.A.L.

Investigation: M.V.K., A.K.B.

Methodology: A.A.L., M.V.K.

Project administration: A.A.L.

Resources: A.A.L., A.K.B.

Supervision: A.A.L.

Validation: A.A.L., M.V.K.

Visualization: M.V.K., A.K.B.

Writing – original draft: A.A.L., A.K.B.

Writing – review & editing: A.A.L.

● Conflict of interest

The authors declare no conflict of interest.

● Additional information

Author IDs:

Artem A. Lobinsky, Scopus ID [56095986600](#);

Maria V. Kaneva, Scopus ID [57202050632](#);

Anastasia K. Bachina, Scopus ID [57199835321](#).

Website:

Ioffe Institute, <https://www.ioffe.ru/ru/>.

References

- Zhu K, Wu T, Sun S, Wen Y, Huang K. Electrode materials for practical rechargeable aqueous Zn-ion batteries: challenges and opportunities. *ChemElectroChem* 2020;7:2714–2734. doi:[10.1002/celec.202000472](#)
- He P, Chen Q, Yan M, Xu X, Zhou L. Building better zinc-ion batteries: a materials perspective. *EnergyChem* 2019;1(3):100022. doi:[10.1016/j.enchem.2019.100022](#)
- Li C, Zhang X, He W, Xu G, Sun R. Cathode materials for rechargeable zinc-ion batteries: From synthesis to mechanism and applications. *J Power Sources*. 2020;449:227596. doi:[10.1016/j.jpowsour.2019.227596](#)
- An G, Hong J, Pak S, Cho Y, Lee S. 2D metal Zn nanostructure electrodes for high-performance Zn ion supercapacitors. *Adv Energy Mater.* 2020;10(3):1902981. doi:[10.1002/aenm.201902981](#)
- Zhang P, Li Y, Wang G, Wang F, Yang S. Zn-ion hybrid micro-supercapacitors with ultrahigh areal energy density and long-term durability. *Adv Mater.* 2019;31(3):1806005. doi:[10.1002/adma.201806005](#)
- Wu S, Chen Y, Jiao T, Zhou J, Cheng J. An aqueous Zn-ion hybrid supercapacitor with high energy density and ultrastability up to 80 000 cycles. *Adv Energy Mater.* 2019;9(47):1902915. doi:[10.1002/aenm.201902915](#)
- Chao D, Fan HJ. Intercalation pseudocapacitive behavior powers aqueous batteries. *Chem.* 2019;5(6):1359–1361. doi:[10.1016/j.chempr.2019.05.020](#)
- Tang H, Yao J, Zhu Y. Recent developments and future prospects for zinc-ion hybrid capacitors: a review. *Adv Energy Mater.* 2021;11(14):2003994. doi:[10.1002/aenm.202003994](#)
- Jin J, Geng X, Chen Q, Ren TL. A better Zn-Ion storage device: Recent progress for Zn-Ion hybrid supercapacitors. *Nano-Micro Lett.* 2022;14:64. doi:[10.1007/s40820-022-00793-w](#)
- Lobinsky A, Kaneva M, Tenevich M, Popkov V. Direct synthesis of Mn₃[Fe(CN)₆]₂·nH₂O nanosheets as novel 2D analog of Prussian Blue and material for high-performance metal-ion batteries. *Micromachines.* 2023;14(5):1083. doi:[10.3390/mi14051083](#)
- Lin Y, Zhang L, Xiong Y, Wei T, Fan Z. Toward the design of high-performance supercapacitors by Prussian Blue, its analogues and their derivatives. *Energy Environ Mater.* 2020;3:323–345. doi:[10.1002/eem2.12096](#)
- Hurlbutt K, Wheeler S, Capone I, Pasta M. Prussian Blue analogs as battery materials. *Joule.* 2018;2:1950–1960. doi:[10.1016/j.joule.2018.07.017](#)
- Cao L-M, Lu D, Zhong D-C, Lu T-B. Prussian blue analogues and their derived nanomaterials for electrocatalytic water splitting. *Coordination Chem Rev.* 2020;407:213156. doi:[10.1016/j.ccr.2019.213156](#)
- Ying S, Chen C, Wang J, Lu C, Liu T, Kong Y, Yi F-Y. Synthesis and applications of Prussian Blue and its analogues as electrochemical sensors. *ChemPlusChem.* 2021;86:1608–1622. doi:[10.1002/cplu.202100423](#)
- Holland A, Kimpton H, Cruden A, Wills R. CuHCF as an electrode material in an aqueous dual-ion Al³⁺/K⁺ ion battery. *Energy Procedia.* 2018;151:69–73. doi:[10.1016/j.egypro.2018.09.029](#)
- Liu S, Pan G-L, Lia G-R, Gao XP. Copper hexacyanoferrate nanoparticles as cathode material for aqueous Al-ion batteries. *J Mater Chem A.* 2015;3:959–962. doi:[10.1039/C4TA04644G](#)
- Song Z, Liu W, Wei X, Zhou Q, Liu H, Zhang Z, Liu G, Zhao Z. Charge storage mechanism of copper hexacyanoferrate nanocubes for supercapacitors. *Chin Chem Lett.* 2020;31(5):1213–1216. doi:[10.1016/j.ccllet.2019.07.022](#)
- Yilmaz G, Tan CF, Hong M, Ho GW. Functional defective metal-organic coordinated network of mesostructured nanoframes for enhanced electrocatalysis. *Adv Funct Mater.* 2018;28:1704177. doi:[10.1002/adfm.201704177](#)
- Shen L, Zhang Q, Luo J, Fu HC, Chen XH, Wu LL, Luo HQ, Li NB. Fabrication of 2D/3D hierarchical PBA and derivative electrocatalysts for overall water splitting. *Appl Surf Sci.* 2021;551:149360. doi:[10.1016/j.apsusc.2021.149360](#)
- Yin J, Zhou J, Wang Y, Ma Y, Zhou X, Wang G, Yang Y, Lu P, Yu J, Chen Y, Yuan Y, Ye C, Xi S, Fan Z. Controlled synthesis of 2D Prussian Blue analog nanosheets with low coordinated water content for high-performance lithium storage. *Small Methods.* 2022;2201107. doi:[10.1002/smt.202201107](#)
- Liu T, Wang J, Jiang Q, Chai N, Ying S, Konga Y, Yi F-Y. One-step synthesis of 2D@3D hollow Prussian blue analogue as a high-performance bifunctional electrochemical sensor. *Dalton Trans.* 2023;52:9048–9057. doi:[10.1039/D3DT00957B](#)
- Wang Y, Ma J, Wang J, Chen S, Wang H, Zhang J. Interfacial scaffolding preparation of hierarchical pba-based derivative electrocatalysts for efficient water splitting. *Adv Energy Mater.* 2019;9:1802939. doi:[10.1002/aenm.201802939](#)
- Biesinger MC, Payne BP, Grosvenor AP, Lau LWM, Gerson AR, Smart RSC. Resolving surface chemical states in XPS analysis of first-row transition metals, oxides and hydroxides: Cr, Mn, Fe, Co and Ni. *Appl Surf Sci.* 2011;257:2717–2730. doi:[10.1016/j.apsusc.2010.10.051](#)
- Song Z, Liub W, Weia X, Zhoua Q, Liub H, Zhang Z, Liu G, Zhao Z. Charge storage mechanism of copper hexacyanoferrate nanocubes for supercapacitors. *Chin Chem Lett.* 2020;31(5):1213–1216. doi:[10.1016/j.ccllet.2019.07.022](#)